6382 J. Med. Chem. 2009, 52, 6382–6393
DOI: 10.1021/jm900941b

Journal of Medicinal Chemistry Article

New 2-Aryloxy-3-phenyl-propanoic Acids As Peroxisome Proliferator-Activated Receptors α/γ Dual Agonists with Improved Potency and Reduced Adverse Effects on Skeletal Muscle Function†

Giuseppe Fracchiolla,[‡] Antonio Laghezza,[‡] Luca Piemontese,[‡] Paolo Tortorella,[‡] Fernando Mazza,[§,∥] Roberta Montanari,[∥] Giorgio Pochetti,[∥] Antonio Lavecchia,[⊥] Ettore Novellino,[⊥] Sabata Pierno,[#] Diana Conte Camerino,[#] and Fulvio Loiodice*[,‡]

[‡]*Dipartimento Farmaco-Chimico, Università degli Studi di Bari, via Orabona 4, 70126 Bari, Italia,* [§]*Dipartimento di Scienze della Salute, Università di L'Aquila, 67010 L'Aquila, Italia,* [∥]*Istituto di Cristallografia, Consiglio Nazionale delle Ricerche, Montelibretti, 00016 Monterotondo Stazione, Roma, Italia,* [⊥]*Dipartimento di Chimica Farmaceutica e Tossicologica, Università degli Studi di Napoli "Federico II", via Montesano 49, 80131 Napoli, Italia, and* [#]*Dipartimento Farmaco-Biologico, Università degli Studi di Bari, via Orabona 4, 70126 Bari, Italia*

Received June 26, 2009

The preparation of a new series of 2-aryloxy-3-phenyl-propanoic acids, resulting from the introduction of a linker into the diphenyl system of the previously reported PPARα/γ dual agonist **1**, allowed the identification of new ligands with improved potency on PPARα and unchanged activity on PPARγ. For the most interesting stereoisomers ***S*-2** and ***S*-4**, X-ray studies in PPARγ and docking experiments in PPARα provided a molecular explanation for their different behavior as full and partial agonists of PPARα and PPARγ, respectively. Due to the adverse effects provoked by hypolipidemic drugs on skeletal muscle function, we also investigated the blocking activity of ***S*-2** and ***S*-4** on skeletal muscle membrane chloride channel conductance and found that these ligands have a pharmacological profile more beneficial compared to fibrates currently used in therapy.

Introduction

Peroxisome proliferator-activated receptors (PPARs[a]) are ligand-activated transcription factors belonging to the nuclear hormone receptor superfamily. They are lipid sensors known to govern numerous biological processes. There are three PPAR subtypes, which are the products of distinct genes and are commonly designated PPARα, PPARγ, and PPARδ. PPARα is highly expressed in the liver and skeletal muscle and is the molecular target for the fibrates (e.g., fenofibrate and gemfibrozil), a class of drugs that lower plasma triglycerides and increase HDL cholesterol levels in humans.[1,2] PPARγ is expressed most abundantly in adipose tissue and mediates the antidiabetic activity of the insulin-sensitizing drugs belonging to the thiazolidindione (TZD) class such as rosiglitazone and pioglitazone.[3] The function of PPARδ is still not fully understood, but recent evidence suggests that this ubiquitously expressed PPAR isoform has pleiotropic actions that may govern diverse physiological processes, including the regulation of lipid and lipoprotein metabolism,[4,5] insulin sensitivity,[6] cardiac function,[7] epidermal biology,[8] neuroprotection,[9] and gastrointestinal tract function and disease.[10] To date, however, no PPARδ agonist has been fully developed and the clinical potential of targeting this isotype remains to be clearly determined. The success of the hypolipidemic fibrates and TZD class of insulin sensitizers has prompted pharmaceutical companies to concentrate on developing more potent and dual agonists acting on these two subtypes. Dual-acting PPARα/γ agonists, in fact, are considered a very attractive option in the treatment of dyslipidemic type 2 diabetes.[11−22] One of the key challenges for the development of a dual agonist is identifying the optimal receptor subtype selectivity ratio. PPARγ full agonists, despite their proven benefits, possess a number of deleterious side effects such as weight gain, peripheral edema, increased risks of congestive heart failure, and higher rate of bone fracture.[23−25] During the past decade, therefore, new drugs acting as partial agonists of PPARγ have been developed with the goal of retaining the beneficial effects while reducing the adverse effects. Metaglidasen (Chart 1), a PPARγ partial agonist, is the most advanced insulin sensitizer that is currently in phase III clinical trials. The results of phase II clinical trials showed that metaglidasen, a prodrug ester that is rapidly and completely modified in vivo to its mature circulating free acid form, significantly improved metabolic parameters without the side effects of fluid retention/edema or weight gain.[24]

Recently, we reported the synthesis and activity of the new ligand **1** (Chart 1) whose structure is related to that of the active metabolite of metaglidasen. This molecule is a dual PPARα/γ ligand with a partial agonism profile toward the γ subtype.[26] The X-ray structure of the complex with PPARγ shows that this ligand occupies a branch, named "diphenyl pocket", of a new L-shaped region of the PPARγ ligand-binding domain (LBD) never sampled before by other known ligands and increases the stabilization of the helix H3, inducing a conformation of the LBD less favorable to the recruitment of coactivators required for full activation of PPARγ.[26] As regards PPARα, the ligand assumes a different orientation

†Protein Data Bank identification number (PDB ID) for PPARγ/***S*-2** and PPARγ/***S*-4** complexes are 3HOD and 3HO0, respectively.

*To whom correspondence should be addressed. Phone: +39 080-5442798. Fax: +39 080-5442231. E-mail: floiodice@farmchim.uniba.it.

[a]Abbreviations: PPAR, peroxisome proliferator-activated receptor; TZD, thiazolidinedione; HDL, high-density lipoprotein; LBD, ligand binding domain; ClC, chloride channel; TBAF, tetrabutylammonium fluoride; DBU, 1,8-diazabicycle[5.4.0]undec-7-ene; EDL, extensor digitorum longus.

 Published on Web 09/23/2009

Chart 1. Chemical Structures of **1**, Metaglidasen, and New PPAR Agonists **2**−**15**

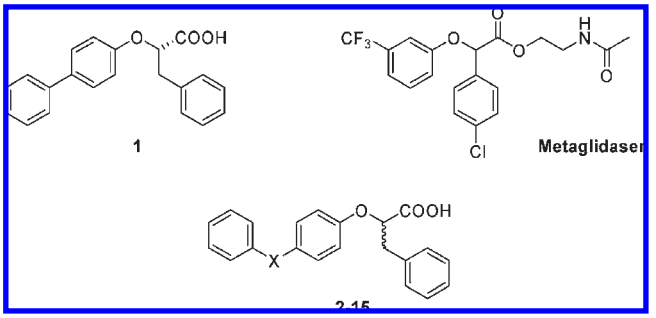

in the LBD that stabilizes better the helices H11 and H12, resulting in a full agonism response. The identification of these novel ligand-receptor interaction modalities represents a new hallmark of the partial agonism behavior of certain ligands and could be exploited for the design of new antidiabetic agents appropriately targeting the PPARs. Since **1** occupies only the first branch of the new L-shaped region, we decided to prepare some analogues characterized by the presence of a linker, with different length and stereoelectronic properties, between the aromatic rings of the diphenyl system that could allow the complete occupation of the entire cavity with the aim of evaluating the effects due to a further stabilization of H11, H12, and the loop 11/12 in terms of potency, efficacy, and subtype selectivity.

For this purpose, we synthesized the new 2-aryloxy-3-phenyl-propanoic acids **2**−**15** reported in Chart 1 and evaluated their PPARα/γ activity. Noteworthy, we identified new ligands with higher potency on PPARα while maintaining basically unchanged the potency and the partial agonism on PPARγ. Considering the high degree of stereoselectivity displayed from these receptors toward the stereoisomer **1**,[26] the influence of the absolute configuration was also taken into account for the most interesting derivatives **2** and **4** bearing one or two methylene groups between the aromatic rings of the diphenyl system, respectively. X-ray studies with PPARγ and docking experiments with PPARα have been performed for the most active isomers ***S*-2** and ***S*-4**, providing a molecular explanation for their different behavior as full and partial agonists of PPARα and PPARγ, respectively. Finally, since skeletal muscle is a target of PPAR agonists, the effects of these two ligands on the function of this tissue were evaluated by measuring the resting chloride conductance (gCl) sustained by the voltage-gated chloride channel ClC-1. Previous studies showed that the reduction of gCl function is one of the mechanisms of action responsible for myopathies, the most important of the complications of lipid-lowering treatment with statins and fibrates.[27−30]

Chemistry

Synthesis of compounds **2**−**5**, **7**, **9**, **11**, **12**, and **14** is depicted in Scheme 1 and was carried out starting from ethyl phenyllactate and the suitable 4-substituted phenol, which were condensed, under Mitsunobu conditions, to obtain the key intermediates **20**−**27**. The saponification of **20**−**26** with 1 N NaOH solution in THF provided the final acids **2**, **3**, **5**, **7**, **9**, **11**, and **12**. Compound **4** was obtained by hydrogenation at 4 atm of **22** in the presence of Wilkinson catalyst followed by saponification of the ester intermediate. The condensation of **27** with ethynylbenzene in the presence of palladium catalyst and TBAF under Sonogashira conditions,[31] followed by saponification of the ester intermediate, led to the final acid **14**. The synthesis of the *R*- and *S*-isomers of compounds **2** and **4** was carried out similarly to the corresponding racemates starting from the readily available (*S*)- or (*R*)-ethyl phenyllactates, respectively. Both enantiomers of acids **2** and **4** had enantiomeric excesses >98% as determined by HPLC analysis on chiral stationary phase (see Experimental Section).

Synthesis of acids **6**, **8**, **10**, **13**, and **15** is represented in Scheme 2 and involved the key intermediate ester **28**, which was prepared from the condensation of 4-hydroxy-benzaldehyde and ethyl phenyllactate according to the procedure reported in Scheme 1. The reduction of the aldehyde group of **28** with $NaBH_4$ at 0 °C afforded the corresponding alcohol whose treatment with PBr_3 yielded **29**. The subsequent condensation of **29** with phenol or thiophenol in the presence of 95% NaH, followed by saponification of the ester intermediates, led to the target compounds **6** and **8**, respectively. For compound **10**, the reductive amination of **28** was carried out with aniline in the presence of bis(triphenylphosphine)copper-(I) borohydride and NH_2SO_3H, following a procedure reported in the literature.[32] The saponification of the corresponding ester intermediate afforded the desired acid. Alternatively, the Wittig reaction of **28** with the commercially available benzyltriphenylphosphonium chloride in the presence of 1,8-diazabicycle[5.4.0]undec-7-ene (DBU) provided the *cis*-ester intermediate of acid **13** as a mixture with the corresponding geometric isomer (53:47, *cis:trans*).[33] The *cis*-isomer was purified by column chromatography and hydrolyzed to give **13**. Following the same procedure, the synthesis of compound **15** was achieved using the phenethyltriphenylphosphonium bromide salt; the hydrogenation in the presence of Wilkinson catalyst of the mixture of propylene geometric isomers so obtained and alkaline hydrolysis of the ester intermediate led to the target compound.

Results and Discussion

Compounds **2**−**15** were evaluated for their agonist activity on the human PPARα (hPPARα) and PPARγ (hPPARγ) subtypes. For this purpose, GAL4-PPAR chimeric receptors were expressed in transiently transfected HepG2 cells according to a previously reported procedure.[34] The results obtained (Table 1) were compared with corresponding data for Wy-14,643 and rosiglitazone used as reference compounds in the PPARα and PPARγ transactivation assays, respectively. The maximum induction obtained with the reference agonist was defined as 100%.

PPARα Activity. The PPARα activity of racemates **2**−**15** was examined first in comparison with **1** and Wy-14,643. The introduction of a methylene between the phenyl rings of **1** afforded the full agonist **2** with a remarkable increase of the potency. A further lengthening of the spacer to ethylene and propylene (compounds **4** and **15**) provided a progressive decrease of potency and efficacy. The introduction of isosteric substitutions into the spacer gave different results: a methylene was better than an oxygen atom (**2** was about four times more potent than **3**), but when the same replacement was carried out on the ethylenic linker, a more or less potent agonist was obtained according to the position of the oxygen atom (**5** was three times as potent as **4**, but **6** about twice less potent than **4**). A similar behavior was observed, even though at reversed positions of the heteroatom, with the introduction of sulfur (compounds **7** and **8**), whereas the

Scheme 1. Synthesis of PPAR Agonists **2**−**5**, **7**, **9**, **11**, **12**, and **14**

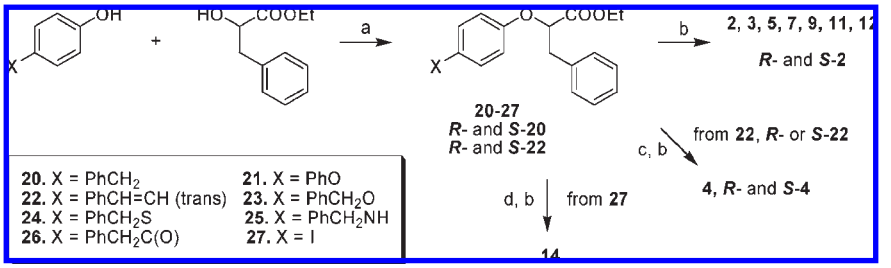

(a) Ph_3P, DIAD, anhydrous THF or toluene, rt; (b) 1 N NaOH/THF (1:1), rt; (c) H_2 (4 atm), Wilkinson cat., THF/MeOH, rt; (d) ethynylbenzene, $PdCl_2(PPh_3)_2$, $(n\text{-butyl})_4NF \cdot xH_2O$, N_2, reflux.

Scheme 2. Synthesis of PPAR Agonists **6**, **8**, **10**, **13**, and **15**

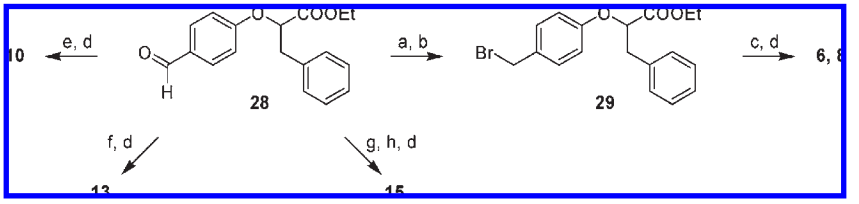

(a) $NaBH_4$, THF/H_2O (1:1), 0 °C; (b) PBr_3, rt; (c) 95% NaH, phenol or thiophenol, anhydrous THF or DMF, N_2, reflux; (d) 1N NaOH/THF (1:1); (e) aniline, $(Ph_3P)_2CuBH_4$, NH_2SO_3H, MeOH, rt; (f) DBU, $PhCH_2(Ph)_3PCl$, anhydrous CH_3CN, N_2, reflux; the isomers mixture was chromatographed on silica gel; (g) DBU, $PhCH_2CH_2(Ph)_3PBr$, anhydrous CH_3CN, N_2, reflux; (h) H_2 (8 atm), Wilkinson cat., THF/EtOH, rt.

Table 1. Activity of the Tested Compounds in Cell-Based Transactivation Assay

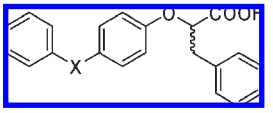

		PPARα		PPARγ	
compd	X	EC_{50} (μM)	efficacy	EC_{50} (μM)	efficacy
1	bond	0.19 ± 0.04	116 ± 4	0.56 ± 0.11	60 ± 8
2	CH_2	0.0159 ± 0.0003	115 ± 27	0.58 ± 0.19	42 ± 1
***R*-2**	CH_2	2.4 ± 0.8	82 ± 2	5.7 ± 0.4	21 ± 1
***S*-2**	CH_2	0.0115 ± 0.0021	107 ± 5	0.572 ± 0.006	40 ± 4
3	O	0.060 ± 0.006	126 ± 6	1.21 ± 0.04	50 ± 5
4	CH_2CH_2	0.33 ± 0.18	86 ± 16	0.86 ± 0.04	39 ± 3
***R*-4**	CH_2CH_2	ia	ia	1.6 ± 0.3	19 ± 4
***S*-4**	CH_2CH_2	0.15 ± 0.04	83 ± 10	0.40 ± 0.20	33 ± 5
5	CH_2O	0.107 ± 0.006	112 ± 8	2.40 ± 0.23	43 ± 1
6	OCH_2	0.60 ± 0.13	107 ± 13	3.0 ± 0.8	40 ± 4
7	CH_2S	0.488 ± 0.017	134 ± 14	1.4 ± 0.4	36 ± 1
8	SCH_2	0.31 ± 0.16	92 ± 17	0.40 ± 0.07	33 ± 3
9	CH_2NH	3.6 ± 1.5	78 ± 4	13 ± 3	27 ± 6
10	$NHCH_2$	1.4 ± 0.4	120 ± 20	9.4 ± 2.3	26 ± 6
11[a]	$CH_2C(O)$	1.8 ± 1.0	106 ± 1	9.1 ± 0.9	40 ± 2
12	CH=CH *trans*	1.75 ± 0.12	57 ± 4	0.72 ± 0.27	50 ± 1
13[a]	CH=CH *cis*	0.160 ± 0.022	107 ± 2	1.5 ± 0.4	34 ± 1
14	C≡C	1.36 ± 0.06	36 ± 3	0.540 ± 0.017	39 ± 1
15	$CH_2CH_2CH_2$	0.72 ± 0.20	67 ± 15	0.87 ± 0.16	30 ± 6
Wy-14,643		1.6 ± 0.3	100 ± 10	ia	ia
rosiglitazone		ia	ia	0.039 ± 0.003	100 ± 9

[a] This compound was tested as sodium salt. ia: inactive at tested concentrations. Efficacy values were calculated as percentage of the maximum obtained fold induction with the reference compounds (Wy-14,643 for PPARα; rosiglitazone for PPARγ).

presence of the amino group afforded agonists (**9**, **10**) with potency in the micromolar range, probably due to the unfavorable capability of this group to function as a hydrogen bond donor. Interesting results were also obtained by substituting the ethylenic spacer of compound **4** with unsaturated two-carbon linkers, which present more constraints with regard to the bond geometry. Among these ligands, the *cis*-derivative **13** was, by far, the most active compound, with a potency 8 and 10 times higher than the acetylene derivative **14** and the ethanoyl and *trans*-ethylene derivatives **11** and **12**, respectively. The importance of stereochemistry was confirmed by evaluating the activity of two enantiomeric pairs:

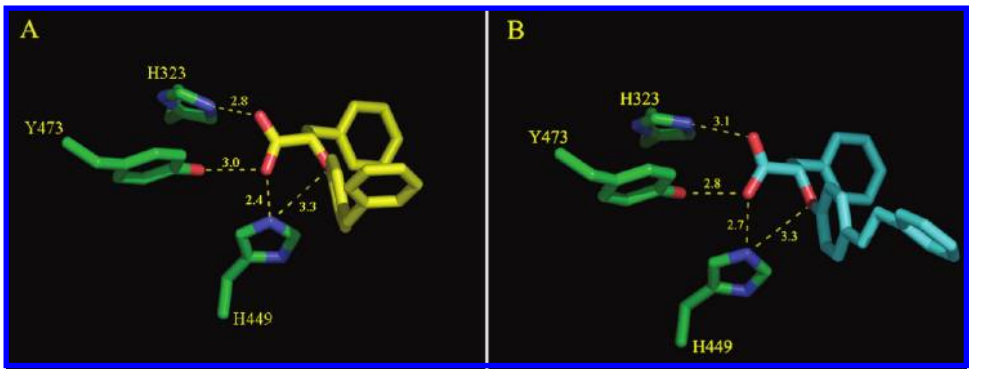

Figure 1. Hydrogen bond network of (A) ***S*-2** (yellow) and (B) ***S*-4** (cyan) in the complex with PPARγ.

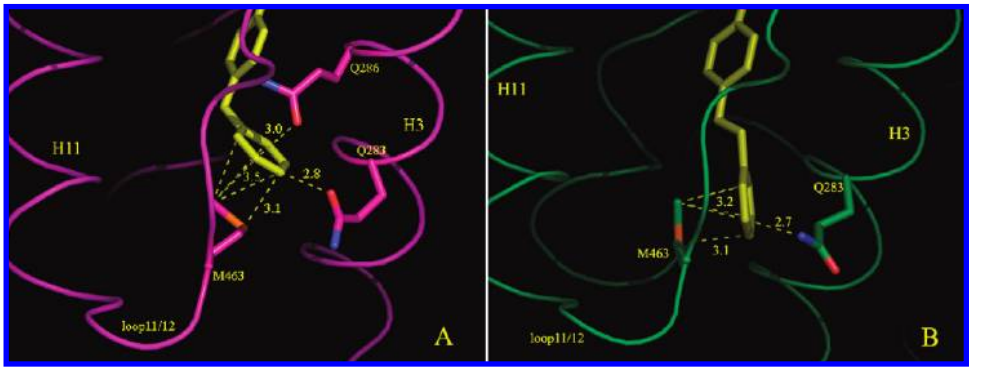

Figure 2. Hydrophobic interactions of (A) ***S*-2** and (B) ***S*-4** in the PPARγ internal cavity. Both ligands are colored in yellow.

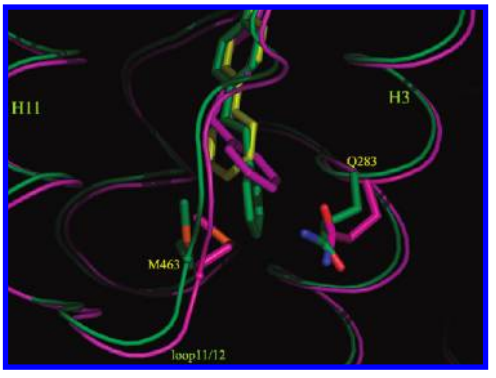

Figure 3. Superposition of the complexes of PPARγ with **1** (yellow), ***S*-2** (purple), and ***S*-4** (green).

***S*-2**, in fact, besides displaying 17-fold improved potency compared to that of **1**, was about 200 times more potent than the corresponding *R*-isomer, whereas ***S*-4** was equipotent with **1** and ***R*-4** was completely inactive.

PPARγ Activity. The PPARγ activity of racemates **2**−**15** was compared with **1** and rosiglitazone. All compounds displayed lower potency than that of rosiglitazone and none of them was able to exhibit full agonist activity. The effects resulting from the introduction of isosteric substitutions into the spacer and its lengthening were basically similar to those on PPARα, whereas a significant change was observed for analogues containing unsaturated two-carbon linkers. The more rigid and planar *trans*-ethylene and acetylene derivatives **12** and **14**, in fact, were more potent than *cis*-derivative **13**, whereas the ethanoyl compound **11** still displayed very low agonist activity. Regarding stereochemistry, the influence of absolute configuration was confirmed also in this case; ***S*-2**, in fact, displayed equipotency with **1** and 10-fold improved potency compared to the corresponding *R*-isomer, whereas ***S*-4** was a little more potent than **1** and four times more potent than ***R*-4**.

With the aim to gain structural biology insight into the role played by the spacer of the diphenyl system of the most active ligands in imparting higher potency on PPARα compared to **1** while maintaining basically unchanged the partial agonism on PPARγ, X-ray crystal studies in PPARγ-LBD and docking experiments in PPARα have been performed for the most active isomers ***S*-2** and ***S*-4**.

Binding of *S*-2 and *S*-4 to PPARγ-LBD. Figure A of the Supporting Information shows the positioning of ***S*-2** and ***S*-4**, respectively, fitted into the electron density map calculated in the hydrophobic pocket of PPARγ. Figure 1 summarizes the binding interactions made by the polar head of ***S*-2** and ***S*-4**, respectively, with the surrounding residues.

In both cases, one of the carboxylate oxygens forms a bifurcated H-bond with the Y473 OH and the H449 $N^{\varepsilon 2}$ groups; the latter group engages the ligand ether oxygen in a further H-bond. The other carboxylate oxygen is at H-bonding distance from H323 $N^{\varepsilon 2}$. The benzyl-phenoxy and phenethyl-phenoxy groups of ***S*-2** and ***S*-4**, respectively, are deeply inserted in the so-called "diphenyl pocket", forming several favorable hydrophobic interactions (see Figure 2).

The bottom of the cavity is delineated by the loop 11/12 and is contoured sidewise by H3 and H11. At the bottom of the cavity, the terminal end of the benzyl-phenoxy and phenethyl-phenoxy groups faces, on one side, the M463 side-chain of the loop 11/12, realizing strong interactions between the methyl and the π-cloud. Electrostatic interactions are realized, on the other side, by the edge of the aromatic ring and the CO group of the Q283 side chain. In the PPARγ/***S*-2** complex, the Q286 side chain is also engaged in such interactions. The short contact between the distal

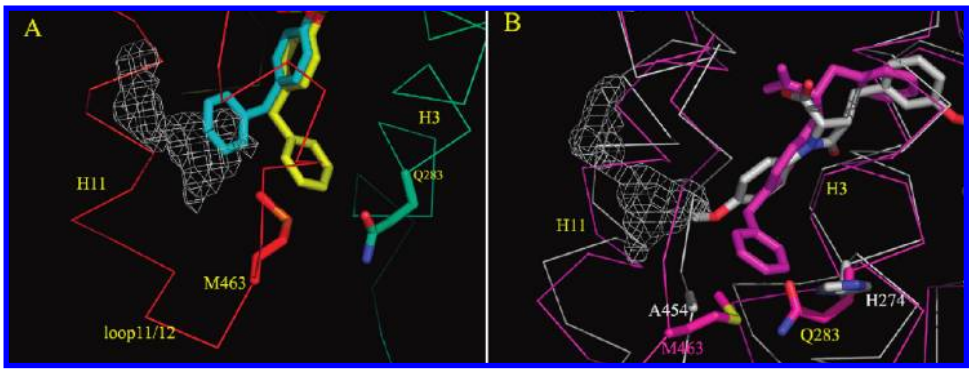

Figure 4. (A) ***S*-2** (yellow), as observed in the crystal complex with PPARγ and its possible orientation (cyan) into the additional space of the diphenyl pocket (white-colored mesh); (B) superposition of the crystal complexes of PPARγ with ***S*-2** (purple) and PPARα with BMS-631707 (white). White-colored mesh represents the additional space of the diphenyl pocket.

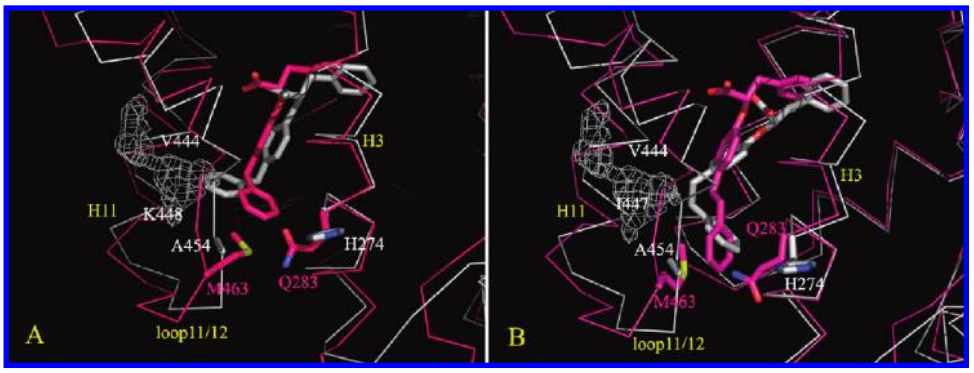

Figure 5. Putative orientation of (A) ***S*-2** (white) docked into the hydrophobic pocket of PPARα, superimposed to the structure of the complex PPARγ/***S*-2** (purple), and (B) ***S*-4** (white) docked into the hydrophobic pocket of PPARα, superimposed to the structure of the complex PPARγ/***S*-4** (purple).

aromatic rings of ***S*-2** and ***S*-4** with M463, Q283, and Q286 are well evidenced by continuous electron density between the interacting groups (see Figure B in the Supporting Information).

Dual Agonism of *S*-2 and *S*-4. The design of these two compounds as well as the other ligands of the series has been made with the aim to prepare analogues of **1** that could occupy the entire "diphenyl pocket" protruding toward H11 and H12. The superposition of the crystal structures of the complexes made by the PPARγ-LBD with the three compounds ***S*-2**, ***S*-4**, and **1** (Figure 3) shows that, despite the greater flexibility of the diphenyl-methylene and diphenyl-ethylene moieties of ***S*-2** and ***S*-4**, respectively, these groups occupy the same portion of the cavity as the diphenyl group of **1**, between H3 and the M463 of the loop 11/12.

Figure 4A shows the possible accommodation of the distal aromatic ring of ***S*-2**, realized by changing the torsional angles between the two aromatic rings, into the additional space of the "diphenyl pocket", calculated by VOIDOO, a program for computing molecular volumes and for studying cavities in proteins.[35] The possibility of this different positioning of ***S*-2** has been confirmed by molecular modeling calculations. The preference of the terminal aromatic rings for adopting the conformations observed in the crystal structures might be ascribed to the strong electrostatic interactions between the π-cloud of the distal aromatic ring and M463 of the loop 11/12 and Q286 of H3. In particular, sulfur-arene interactions are known to be strongly attractive.[36,37] The partial agonism of both compounds toward PPARγ is in accordance with the hypothesis that ligands that better stabilize H3 rather than H11 and H12 lose the character of full agonists.[26]

In Figure 4B, the Cα superposition between the crystal complex of PPARγ/***S*-2** and that of the human PPARα complexed with the α/γ dual agonist BMS-631707 (PDB code 2REW)[38] is shown. It has already been observed[26] that ligands occupying the "diphenyl pocket" in PPARα assume a different slope into the cavity in order to maintain the carboxylate H-bond network because of the longer protrusion of the Y314 side chain (H323 in PPARγ). It is evident from Figure 4B that if ***S*-2** could assume in PPARα the same orientation of BMS-631707, it would occupy the additional space of the "diphenyl pocket" calculated by VOIDOO, protruding toward H11 and H12. Moreover, in PPARα, it would be missing the strong sulfur-arene interactions that could orient the terminal ring between H3 and the loop 11/12, given that there is the A454 residue in place of PPARγ M463 and also H274 in place of Q283.

To test whether a possible occupation of the entire "diphenyl pocket" could be realized by ***S*-2** and ***S*-4** at the PPARα-LBD, the binding mode of both compounds was investigated by docking experiments. To this end, again, the crystal structure of PPARα/BMS-631707 was employed. The ligand-receptor complexes were predicted through the automated docking software GOLD 4.0,[39,40] which in several studies was shown to yield better performances compared to other similar programs.[41−44] The GoldScore-CS docking protocol[45] was adopted in this study. In this protocol, the poses obtained with the original GoldScore function are rescored and reranked with the GOLD implementation

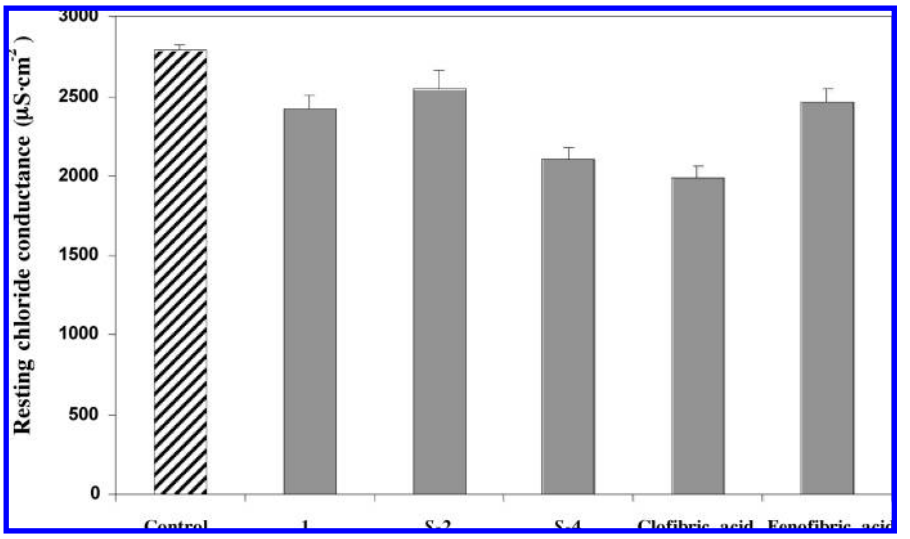

Figure 6. Effects of in vitro application of **1**, ***S*-2**, ***S*-4**, clofibric acid, and fenofibric acid on gCl of rat EDL muscle. All compounds were tested at 100 μM concentration. Each bar represents the mean ± SEM of gCl from 10−36 fibers. Student's *t* test showed significant differences between all treated groups and the control group ($P < 0.02$ or less).

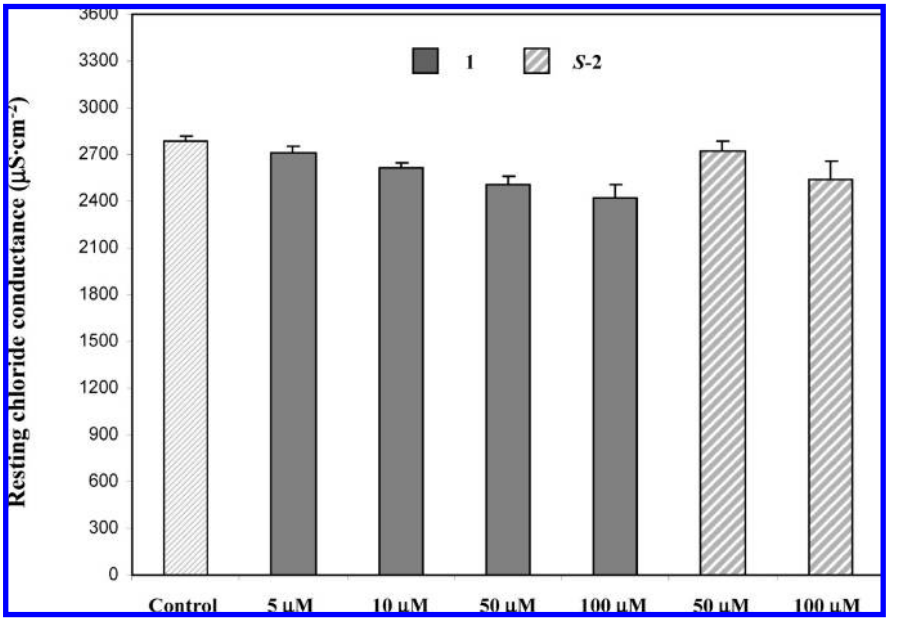

Figure 7. Dose-dependent effects of **1** and ***S*-2** on gCl of rat EDL muscle. Each bar represents the mean ± SEM of gCl from 6−36 fibers. Student's *t* test showed significant differences between all treated groups and the control group ($P < 0.05$ or less).

of the ChemScore function.[45,46] When ***S*-2** and ***S*-4** were docked within the PPARα binding site, about 60% of the conformations generated by GOLD adopted only one highly conserved orientation. Figure 5A shows the putative orientation of ***S*-2** into the hydrophobic pocket of PPARα in comparison with the structure of the complex PPARγ/***S*-2**. The ligand assumes a position very similar to that of BMS-631707, with the distal aromatic ring approaching helix 11 through vdW interactions with V444 and K448; at the same time, this ring interacts with the residues A454, A455, and L456 of the loop 11/12. The stabilization of H11, the loop 11/12, and indirectly, H12, upon ligand binding could explain the nanomolar activity of ***S*-2** and its character of full agonist toward PPARα. It is interesting to notice that the terminal ring of ***S*-2** occupies, as expected, part of the additional volume of the diphenyl pocket, calculated by VOIDOO. Additional substitutions on this ring could better fill this volume with a further stabilization of H11 and H12. The preparation of ***S*-2** analogues characterized by the presence on this phenyl of groups with different stereoelectronic properties is under way.

Figure 5B shows ***S*-4** docked into the LBD of PPARα. The comparison of this structure with that of the complex PPARγ/***S*-4** evidence a similar position of the terminal aromatic ring between H3 and the loop 11/12, with vdW interactions with A454 and A455 of this loop and with the residues V270, H274, and Q277 of H3. However, the shifted position in PPARα toward H11 of the ethylene linker between the two phenyl groups permits the interaction of this moiety with the residues V444 and I447 of this helix. This could explain the almost full agonism of ***S*-4** toward PPARα, with a small loss of potency and efficacy due to the maintained

contacts with the H3. Also, this case reinforces the hypothesis that a stabilization of H3 could attenuate the full agonist character of a ligand.

Effects of 1, *S*-2, and *S*-4 on Skeletal Muscle Chloride Conductance. Lipid-lowering drugs show diffuse myopathies more frequently than other drugs.[29] They start with myalgia, malaise, and muscle tenderness, followed by elevated plasma levels of muscular enzymes.[47] Extreme fatigue may also be a leading symptom, and pain may be present or absent. Rhabdomyolysis is the most feared side effect in the clinical use of lipid lowering medications, particularly of statins. These, either alone or particularly when associated with fibrates, may give rise to significant muscle necrosis.[48] Since the first description of muscular lesions after clofibrate therapy,[49] myopathies have been attributed to all lipid-lowering drugs: nicotinic acid,[50] fibrates,[51−53] and statins.[54] Myopathy as adverse drug reaction of lipid-lowering drugs has been characterized biochemically and morphologically, and there exist a few mechanistic hypotheses.[29] Our previous studies allowed the identification of the resting chloride conductance (gCl), sustained by the voltage-gated chloride channel ClC-1, as a cellular target of statins and fibrates action.[30] ClC-1 is a muscle-specific channel that controls membrane electrical stability and functional processes such as excitation and contraction. A reduced ClC-1 function causes disorders related to abnormal action potential firing. Patch clamp studies have demonstrated a direct inhibition of human ClC-1 channel expressed in cultured HEK cells by fenofibric acid.[55] On this basis, we decided to test **1**, ***S*-2**, and ***S*-4** to evaluate the possibility that these fibrate-like drugs were able, in the same way, to interfere with the chloride ion flux of skeletal muscle membrane.

The effects of in vitro application of these compounds on gCl of rat extensor digitorum longus (EDL) muscle are shown in Figure 6 in comparison with clofibric acid and fenofibric acid, active metabolites of clofibrate and fenofibrate, respectively. In this experiment, we tested all compounds at 100 μM concentration and found that **1** and ***S*-2** were poorly effective, producing only a 12% and 9% decrease of gCl, respectively, similar to fenofibric acid (11%). ***S*-4** exhibited a little higher potency, producing a 24% block of gCl similar to 28% block due to clofibric acid. In a second experiment, we evaluated the effects on gCl produced from lower doses of **1** and ***S*-2**.

As shown in Figure 7, the block activity of the former vanished at 5 μM (~2%), whereas the latter was basically inactive even at 50 μM (~2%). All compounds were ineffective on resting potassium conductance (gK). These data indicate that our compounds are potentially much safer than fibrates currently used in therapy. In fact, even though similar in blocking activity of gCl at the tested concentrations, **1**, ***S*-2**, and ***S*-4** display a potent PPAR agonist activity at much lower doses than those of clinically used fibrates. ***S*-2**, particularly, is about 3000 and 500 times as potent as fenofibric acid on PPARα and PPARγ, respectively (EC_{50} of fenofibric acid: 30 μM on PPARα and 300 μM on PPARγ).[12]

Conclusion

In conclusion, the introduction of a linker into the diphenyl system of compound **1**, previously reported as a PPARα/γ dual agonist, allowed the identification of new ligands with improved potency on PPARα and unchanged partial agonist activity on PPARγ. For the most interesting stereoisomers ***S*-2** and ***S*-4**, X-ray studies in PPARγ and docking studies in PPARα provided a molecular explanation for their different behavior as full and partial agonists of PPARα and PPARγ, respectively. Moreover, the blocking activity of these two ligands on skeletal muscle chloride conductance, which is related to myopathies frequently observed in the treatment with lipid-lowering drugs, resulted in a profile more beneficial than fibrates currently used in therapy. The high potency on PPARα as well as the partial agonism on PPARγ and the poor activity on skeletal muscle function allow, therefore, the claim that these new molecules may represent the leads of a potentially safer class of drugs with better therapeutic effects in the treatment of type 2 diabetes.

Experimental Section

Chemical Methods. Column chromatography was performed on ICN silica gel 60 Å (63−200 μm) as a stationary phase. Melting points were determined in open capillaries on a Gallenkamp electrothermal apparatus and are uncorrected. Mass spectra were recorded with a HP GC/MS 6890−5973 MSD spectrometer, electron impact 70 eV, equipped with HP chemstation. ^{1}H NMR spectra were recorded in $CDCl_3$ (the use of DMSO-d_6 or CD_3OD as a solvent is specified) on a Varian-Mercury 300 (300 MHz) spectrometer at room temperature (20 °C). Chemical shifts are expressed as parts per million (δ). For optical isomers, MS and ^{1}H NMR spectra are reported only for the racemate or one of the two enantiomers. Microanalyses of solid compounds were carried out with an Eurovector Euro EA 3000 model analyzer; the analytical results are within ±0.4% of theoretical values. Only for final compounds **4**, ***S*-4**, and **12** the data related to carbon are +0.42%, −0.43%, and −0.45%, respectively. Optical rotations were measured with a Perkin-Elmer 341 polarimeter at room temperature (20 °C): concentrations are expressed as g (100 mL)$^{-1}$. The enantiomeric excesses of acids were determined by HPLC analysis of their methyl esters, obtained by reaction with a solution of diazomethane in Et_2O, on Chiralcel OD column (4.6 mm i.d. × 250 mm, Daicel Chemical Industries, Ltd., Tokyo, Japan). Analytical liquid chromatography was performed on a PE chromatograph equipped with a Rheodyne 7725i model injector, a 785A model UV/vis detector, a series 200 model pump, and NCI 900 model interface. Chemicals were obtained from Aldrich (Milan, Italy), Lancaster (Milan, Italy), or Acros (Milan, Italy) and were used without any further purification.

Preparation of 4-(Benzylthio)phenol. A solution of benzylbromide (1.35 g, 7.9 mmol) in $CHCl_3$ (20 mL) was added dropwise to a mixture of 4-mercaptophenol (1.0 g, 7.9 mmol) and Et_3N (1.2 g, 11.85 mmol). The reaction mixture was stirred at reflux for 1.5 h, then washed with NH_4Cl saturated solution. The organic layer was dried over Na_2SO_4, filtered, and evaporated to dryness, affording the title compound as a yellow solid in quantitative yield. This product was used in the next step without any further purification.

General Procedure for the Preparation of Ethyl 2-(4-Substituted-phenoxy)-3-phenyl-propanoates (20−27, *R*- and *S*-20, *R*- and *S*-22 in Scheme 1 and 28 in Scheme 2). A solution of diisopropylazodicarboxylate (DIAD, 10 mmol) in anhydrous THF or toluene (20 mL) was added dropwise to an ice-bath cooled mixture of ethyl phenyllactate (10 mmol), the appropriate phenol (10 mmol), and triphenylphosphine (10 mmol) dissolved in the same anhydrous solvent (50 mL). The reaction mixture was stirred at room temperature overnight, under N_2 atmosphere. The organic solvent was evaporated in vacuo, and a mixture of Et_2O and *n*-hexane (40 mL, 1:1) was added to the residue. The resulting precipitate was filtered off, and the filtrate was evaporated to dryness. The residue was chromatographed on a silica gel column (petroleum ether/ethyl acetate 9:1 as eluent),

affording the desired compounds as oils or white solids in 32−77% yields.

Both enantiomers of compounds **20** and **22** were prepared with the same procedure starting from *R*- or *S*-ethyl phenyllactate in 35−42% yields.

Ethyl 2-(4-Benzyl-phenoxy)-3-phenyl-propanoate (20). Colorless oil; 32% yield.

Ethyl 2-(4-Phenoxy−phenoxy)-3-phenyl-propanoate (21). Yellow oil; 69% yield.

Ethyl 2-(4-*trans*-Styryl-phenoxy)-3-phenyl-propanoate (22). White solid; 38% yield.

Ethyl 2-(4-Benzyloxy-phenoxy)-3-phenyl-propanoate (23). White solid; 34% yield.

Ethyl 2-(4-Benzylthio-phenoxy)-3-phenyl-propanoate (24). Colorless oil; 45% yield.

Ethyl 2-(4-Benzylamino-phenoxy)-3-phenyl-propanoate (25). Yellow oil; 33% yield.

Ethyl 2-(4-Phenylacetyl-phenoxy)-3-phenyl-propanoate (26). Colorless oil; 60% yield.

Ethyl 2-(4-Iodo-phenoxy)-3-phenyl-propanoate (27). White solid; 77% yield.

Ethyl 2-(4-Formyl-phenoxy)-3-phenyl-propanoate (28). Colorless oil; 68% yield.

Preparation of Ethyl 2-(4-Phenethyl-phenoxy)-3-phenyl-propanoate (Scheme 1, Step c). A solution of **22** (0.280 g, 0.75 mmol) in THF (20 mL) was added to a stirred suspension of Wilkinson catalyst (35 mg, 0.0375 mmol) in abs EtOH (2 mL). The resulting mixture was stirred at room temperature under H_2 atmosphere (4 atm) for 20 h. The suspension was filtered through a celite pad to remove the catalyst and the solvent was evaporated to dryness, obtaining a dark solid residue, which was chromatographed on a silica gel column (petroleum ether/ethyl acetate 95:5 as eluent), affording the desired compound as a colorless oil in 70% yield. Both enantiomers of the title compound were prepared with the same procedure starting from ***R***- or ***S*-22** in 70−73% yields.

Preparation of Ethyl 2-(4-Phenylethynyl-phenoxy)-3-phenyl-propanoate (Scheme 1, Step d). A mixture of **27** (0.930 g, 2.35 mmol), phenylacetylene (0.300 g, 2.82 mmol), $PdCl_2(PPh_3)_2$ (0.045 g, 0.07 mmol), and tetrabutylammonium fluoride hydrate (1.84 g, 7.05 mmol) was refluxed, under N_2 atmosphere, for 17 h. Then, Et_2O (10 mL) and H_2O (10 mL) were added to the mixture and the organic phase was washed with brine, dried over Na_2SO_4, and filtered. The solvent was evaporated to dryness, affording a brown oil residue, which was chromatographed on a silica gel column (petroleum ether/ethyl acetate 95:5 as eluent) to give the desired compound as a yellow oil in 15% yield.

Preparation of 29 (Scheme 2). $NaBH_4$ (0.145 g, 3.85 mmol) was added to a stirred and ice-bath cooled solution of **28** (1.044 g, 3.50 mmol) in THF (40 mL) and H_2O (40 mL). The reaction mixture was stirred for 0.5 h at 0 °C and, after distilling off the organic solvent, the aqueous residue was added with H_2O and ice then extracted with Et_2O. The organic phase was washed with 10% Na_2CO_3 and brine. The organic solvent was dried over Na_2SO_4, filtered, and evaporated in vacuo, affording the ethyl 2-(4-hydroxymethyl-phenoxy)-3-phenyl-propanoate as a pale-yellow oil in 91% yield. GC/MS, *m*/*z* (%): 300 (73) [M^+], 135 (100) [$C_9H_{11}O^+$]. PBr_3 (0.810 g, 3.00 mmol) was carefully added to this intermediate (0.901 g, 3.00 mmol) at 0 °C. The reaction mixture was stirred for 5 h at room temperature, then poured onto ice and extracted with Et_2O. The organic layer was washed with brine, dried over Na_2SO_4, and filtered. The solvent was evaporated to dryness, affording a solid residue which was chromatographed on a silica gel column (petroleum ether/ethyl acetate 90:10 as eluent) to give the title compound in 66% yield.

Preparation of Ethyl 2-(4-Phenoxymethyl-phenoxy)- and 2-(4-Pheylthiomethyl-phenoxy)-3-phenyl-propanoates (Scheme 2, Step c). An ice-bath cooled suspension of NaH (95% powder, 1.1 mmol) in anhydrous THF (6 mL) was carefully added with phenol or thiophenol (1.1 mmol) under nitrogen atmosphere. After 0.5 h, a solution of **29** (0.28 mmol) in anhydrous THF (4 mL) was added dropwise to the reaction mixture, which was refluxed for 5 h. After distilling off the organic solvent, the residue was treated with ice and extracted with Et_2O. The organic layer was washed with NH_4Cl saturated solution, 0.5 N NaOH and brine, dried over Na_2SO_4, and filtered. The solvent was evaporated in vacuo to give a residue, which was chromatographed on a silica gel column (petroleum ether/ethyl acetate 95:5 as eluent), affording the desired compounds as pale-yellow oils.

Ethyl 2-(4-Phenoxymethyl-phenoxy)-3-phenyl-propanoate. Yield 67%.

Ethyl 2-(4-Phenylthiomethyl-phenoxy)-3-phenyl-propanoate. Yield 47%.

Preparation of Ethyl 2-(4-Phenylaminomethyl-phenoxy)-3-phenyl-propanoate (Scheme 2, Step e). Aniline (0.217 g, 2.3 mmol) and sulfamic acid (0.224 g, 2.3 mmol) were added to a solution of **28** (0.841 g, 2.80 mmol) in CH_3OH (20 mL). After 0.5 h, $(Ph_3P)_2CuBH_4$ (1.53 g, 2.5 mmol) was carefully added to the mixture. After 15 h at room temperature, the solvent was removed under reduced pressure and the residue dissolved in ethyl acetate. The organic phase was washed with 1 N HCl, 0.5 N NaOH, and with brine, then was dried over Na_2SO_4 and filtered. The solvent was evaporated to dryness, affording an oily residue which was chromatographed on a silica gel column (petroleum ether/ethyl acetate 90:10 as eluent) to give the desired compound as a yellow oil (1.26 mmol) in 56% yield.

Preparation of Ethyl 2-(4-*cis*-Styryl-phenoxy)-3-phenyl-propanoate (Scheme 2, Step f). To a stirred solution of benzyltriphenylphosphonium chloride (3.01 g, 7.72 mmol) in anhydrous CH_3CN (15 mL) a solution of **28** (1.54 g, 5.15 mmol) in anhydrous CH_3CN (12 mL) was carefully added, under N_2 atmosphere. After 0.5 h, a solution of DBU (1.19 g, 7.72 mmol) in anhydrous CH_3CN (13 mL) was added to the reaction mixture, which was refluxed for 5 h. The solvent was removed under reduced pressure and the residue dissolved in ethyl acetate. The organic phase was washed with NH_4Cl saturated solution and twice with brine, then was dried over Na_2SO_4 and filtered. The solvent was evaporated to dryness, affording an oily mixture of the two stereoisomers which were chromatographed on a silica gel column (petroleum ether/ethyl acetate 98:2). The title compound was obtained as a yellow oil in 19% yield.

Preparation of Ethyl 2-[4-(3-Phenyl-propyl)phenoxy]-3-phenyl-propanoate (Scheme 2, Steps g and h). Following the same procedure reported above, the reaction of **28** with phenethyltriphenylphosphonium bromide afforded *cis*- and *trans*-ethyl 2-[4-(3-phenyl-propenyl)phenoxy]-3-phenyl-propanoates in 26% yield. The resultant mixture of stereoisomers (0.505 g, 1.32 mmol) was dissolved in THF (25 mL) and added to a suspension of Wilkinson catalyst (0.070 g) in abs EtOH (20 mL). The mixture was stirred at room temperature under H_2 atmosphere (8 atm). After 6 h, the suspension was filtered through a celite pad to remove the catalyst and the filtrate was concentrated under reduced pressure to give a brown oil which was chromatographed on a silica gel column (petroleum ether/ethyl acetate 80:20 as eluent), affording the title compound as a colorless oil (0.503 g, 1.30 mmol) in 98% yield.

Preparation of the Final Acids 2−15. General Procedure (Schemes 1 and 2). A solution of the corresponding ethyl ester (5 mmol) in THF (30 mL) and 1 N NaOH (30 mL) was stirred for 2−24 h at room temperature. The organic solvent was removed under reduced pressure, and the aqueous phase was acidified with 6 N HCl and extracted with ethyl acetate. The combined organic layers were dried over Na_2SO_4 and evaporated to dryness, affording the final acids in quantitative yields as white solids or colorless oils.

2-(4-Benzyl-phenoxy)-3-phenyl-propanoic Acid (2). Yield 48%.

(*S*)-2-(4-Benzyl-phenoxy)-3-phenyl-propanoic Acid (*S*-2). Yield 32%.

(*R*)-2-(4-Benzyl-phenoxy)-3-phenyl-propanoic Acid (*R*-2). Yield 56%.

2-(4-Phenoxy-phenoxy)-3-phenyl-propanoic Acid (3). Yield 94%.

2-(4-Phenethyl-phenoxy)-3-phenyl-propanoic Acid (4). Yield 74%.

(*S*)-2-(4-Phenethyl-phenoxy)-3-phenyl-propanoic Acid (*S*-4). Yield 40%.

(*R*)-2-(4-Phenethyl-phenoxy)-3-phenyl-propanoic Acid (*R*-4). Yield 40%.

2-(4-Benzyloxy-phenoxy)-3-phenyl-propanoic Acid (5). Yield 58%.

2-(4-Phenoxymethyl-phenoxy)-3-phenyl-propanoic Acid (6). Yield 67%.

2-(4-Benzylthio-phenoxy)-3-phenyl-propanoic Acid (7). Yield 67%.

2-(4-Phenylthiomethyl-phenoxy)-3-phenyl-propanoic Acid (8). Yield 52%.

2-(4-Benzylamino-phenoxy)-3-phenyl-propanoic Acid (9). Yield 24%.

2-(4-Phenylaminomethyl-phenoxy)-3-phenyl-propanoic Acid (10). Yield 77%.

2-(4-*trans*-Styryl-phenoxy)-3-phenyl-propanoic Acid (12). Yield 68%.

2-(4-Phenylethynyl-phenoxy)-3-phenyl-propanoic Acid (14). Yield 70%.

2-[4-(3-Phenyl-propyl)phenoxy]-3-phenyl-propanoic Acid (15). Yield 57%.

Compounds **11** and **13** were tested as sodium salts, obtained after reaction of the corresponding acid (1 mmol) with $NaHCO_3$ (1 mmol) in 95% EtOH (10 mL) and water (1 mL). Then the solvent was distilled off and the resulting white solid was washed many times with Et_2O.

2-(4-Phenylacetyl-phenoxy)-3-phenyl-propanoic Acid Sodium Salt (11). Yield 89%.

2-(4-*cis*-Styryl-phenoxy)-3-phenyl-propanoic Acid Sodium Salt (13). Yield 67%.

Protein Expression, Purification, and Crystallization. The LBD of PPARγ was expressed as N-terminal His-tagged protein using a pET28 vector and purified as previously described.[56] Crystals of apo-PPARγ were obtained by vapor diffusion at 20 °C using a sitting drop made by mixing 2 μL of protein solution (15 mg/mL, in 20 mM Tris, DTT 5 mM, 0.5 mM EDTA, pH 8.0) with 2 μL of reservoir solution (0.8 M NaCitrate, 0.15 mM Tris, pH 8.0). The crystals were soaked for 7 days in a storage solution (1.2 M NaCitrate, 0.15 M Tris, pH 8.0) containing the ligands (0.1 mM). The ligands dissolved in DMSO were diluted in the storage solution so that the final DMSO concentration was 0.5%. The storage solution with glycerol 20% (v/v) was used as cryoprotectant. Crystals of PPARγ/***S*-4** and PPARγ/***S*-2** belong to the space group *C*2 with cell parameters shown in Table 1 of the Supporting Information. The asymmetric unit is formed by one homodimer.

Structure Determination. X-ray data were collected at 100 K under a nitrogen stream using synchrotron radiation (beamline ID14−2 at ESRF, Grenoble). The diffracted intensities were processed using the programs MOSFLM and SCALA[57] for both complexes. Refinements were performed with CNS[58] using the coordinates of PPARγ/**1**[26] (PDB code 3B3K) as a starting model. All data between 8−2.6 Å were included for PPARγ/***S*-4** (between 8−2.1 Å, for PPARγ/***S*-2**). The statistics of crystallographic data and refinement are summarized in Table 1 of the Supporting Information. The coordinates of PPARγ/***S*-2** and PPARγ/***S*-4** complexes have been deposited in the Brookhaven Protein Data Bank (PDB) with the codes 3HOD and 3HO0, respectively.

Computational Chemistry. Molecular modeling and graphics manipulations were performed using the molecular operating environment (MOE)[59] and UCSF-CHIMERA software packages,[60] running on a 2 CPU (PIV 2.0−3.0 GHZ) Linux workstation. Energy minimizations were realized by employing the AMBER 9 program,[61] selecting the Cornell et al. force field.[62]

Ligand and Protein Setup. The core structures of compounds ***S*-2** and ***S*-4** were constructed using standard bond lengths and bond angles of the MOE fragment library. The carboxylate group was taken as dissociated. Geometry optimizations were accomplished with the MMFF94X force field, available within MOE. The coordinates of PPARα in complex with the α/γ dual agonist BMS-631707 (PDB code 2REW),[38] recovered from Brookhaven Protein Database,[63] were used in the docking experiments. Bound ligand and water molecules were removed. A correct atom assignment for Asn, Gln, and His residues was done, and hydrogen atoms were added using standard MOE geometries. Partial atomic charges were computed by MOE using the AMBER99 force field. All heavy atoms were then fixed, and hydrogen atoms were minimized using the AMBER99 force field and a constant dielectric of 1, terminating at a gradient of 0.001 kcal mol^{-1} $Å^{-1}$.

Docking Simulations. Docking of BMS-631707, ***S*-2** and ***S*-4** to PPARα was performed with GOLD 4.0 version,[39,40] which uses a genetic algorithm for determining the docking modes of ligands and proteins. An advantage of GOLD over other docking methods is the program's ability to account for some rotational protein flexibility as well as full ligand flexibility. Specifically, OH groups of Ser, Thr, and Tyr, and amino groups of Lys are allowed to rotate during docking to optimize H-bonding to the ligand. GOLD requires a user-defined binding site. It searches for a cavity within the defined area and considers all the solvent-accessible atoms in that area as active-site atoms. The fitness score function that was implemented in GOLD (GoldScore) is made up of four components that account for protein−ligand binding energy: protein−ligand hydrogen bond energy (external H-bond), protein−ligand van der Waals energy (external vdW), ligand internal vdW energy (internal vdW), and ligand torsional strain energy (internal torsion). Parameters used in the fitness function (hydrogen bond energies, atom radii and polarizabilities, torsion potentials, hydrogen bond directionalities, and so forth) are taken from the GOLD parameter file. The fitness score is taken as the negative of the sum of the energy terms, so larger fitness scores indicated better bindings. The fitness function has been optimized for the prediction of ligand binding positions rather than the prediction of binding affinities, although some correlation with the latter can be also found.[45] The protein input file may be the entire protein structure or a part of it comprising only the residues that are in the region of the ligand binding site. In the present study, GOLD was allowed to calculate interaction energies within a sphere of a 18 Å radius centered on the OH atom of Y464 in the PPARα structure. The Goldscore-CS docking protocol[45] was adopted in this study. To perform a thorough and unbiased search of the conformation space, each docking run was allowed to produce 200 poses without the option of early termination, using standard default settings. With the aim to test the validity of the Goldscore-CS docking protocol for the human PPARα system, BMS-631707, the cocrystallized ligand, was first docked back into its binding site. In this docking run, the 200 poses produced by GOLD resulted in only one prevailing cluster on the basis of their conformations: 90 of the poses closely resembled the cocrystallized conformation with a heavy atom root-mean-square deviation (rmsd) ranging from 0.4 to 1.4 Å. ChemScore was able to rank 30 out of the 90 poses from this cluster as the highest ranked 13 poses. Thus, this docking protocol was considered to be suitable for the subsequent docking runs for compounds ***S*-2** and ***S*-4**.

The top solution obtained after reranking of the poses with ChemScore (ChemScore fitness = 45.9 kJ mol^{-1} for ***S*-2** and 44.4 kJ mol^{-1} for ***S*-4**) was selected to generate the PPARα/ligand complexes.

Energy Refinement of the Ligand/Receptor Complexes. To eliminate any residual geometric strain, the obtained complexes were energy minimized for 5000 steps using combined steepest descent and conjugate gradient methods until a convergence

value of 0.001 kcal mol^{-1} $Å^{-1}$. Upon minimization, the protein backbone atoms were held fixed. Geometry optimizations were performed using the SANDER module in the AMBER suite of programs, employing the Cornell et al. force field to assign parameters for the standard amino acids. General AMBER force field (GAFF) parameters were assigned to ligands, while the partial charges were calculated using the AM1-BCC method as implemented in the ANTECHAMBER suite of AMBER.

Biological Methods. Medium, other cell culture reagents, and Wy-14,643 were purchased from Sigma (Milan, Italy). BRL 49653 (rosiglitazone) was obtained by Hefei Scenery Chemical Co. (Hefei, Anhui, People's Republic of China). Clofibric acid and fenofibric acid were obtained by hydrolysis of fenofibrate and clofibrate (Sigma Aldrich, Italy), respectively.

Plasmids. The expression vectors expressing the chimeric receptors containing the yeast GAL4-DNA binding domain fused to the human PPARα or PPARγ ligand binding domain (LBD), and the reporter plasmid for these GAL4 chimeric receptors (pGAL5TKpGL3) containing five repeats of the GAL4 response elements upstream of a minimal thymidine kinase promoter that is adjacent to the luciferase gene were described previously.[64]

Cell Culture and Transfections. Human hepatoblastoma cell line HepG2 (Interlab Cell Line Collection, Genoa, Italy) was cultured in minimum essential medium (MEM) containing 10% of heat-inactivated foetal bovine serum, 100 U penicillin $G \cdot mL^{-1}$, and 100 μg streptomycin sulfate$\cdot mL^{-1}$ at 37 °C in a humidified atmosphere of 5% CO_2. For transactivation assays, 10^5 cells per well were seeded in a 24-well plate and transfections were performed after 24 h with CAPHOS (Sigma, Milan, Italy), a calcium-phosphate method, according to the manufacturer's guidelines. Cells were transfected with expression plasmids encoding the fusion protein GAL4-PPARα LBD or GAL4-PPARγ LBD (30 ng), pGAL5TKpGL3 (100 ng), pCMVβgal (250 ng). Four hours after transfection, cells were treated for 20 h with the indicated ligands in triplicate. Luciferase activity in cell extracts was then determined by a luminometer (VICTOR^3 V Multilabel Plate Reader, PerkinElmer). β-Galactosidase activity was determined using β-D-galactopyranoside (Sigma, Milan, Italy) as described previously.[65] All transfection experiments were repeated at least twice.

Electrophysiological Recordings of Resting Membrane Chloride Conductance. The electrophysiological recordings were done in vitro on the extensor digitorum longus (EDL) muscle dissected from adult Wistar male rats (Charles River Laboratories, Calco, Italy) under urethane anesthesia (1.2 g kg^{-1} ip). Soon after the dissection, rats still anaesthetized were euthanized with a urethane overdose. All experimental protocols were carried out in accordance with the Guide for the care and use of laboratory animals. The EDL muscles were immediately placed in a 25 mL bath chamber, maintained at 30 °C, and perfused with normal or chloride-free physiological solution (gassed with 95% O_2 and 5% CO_2; pH = 7.2−7.3).[30] The normal (chloride containing) physiological solution had the following composition (in mM): 148 NaCl, 4.5 KCl, 2 $CaCl_2$, 1 $MgCl_2$, 12 $NaHCO_3$, 0.44 NaH_2PO_4, 5.5 glucose. The chloride free solution was made by equimolar substitution of methylsulfate salts for NaCl and KCl and nitrate salts for $CaCl_2$ and $MgCl_2$. Using the two-intracellular-microelectrodes technique, in current clamp mode, the membrane resistance (R_m) and the fiber diameter were calculated. These parameters were obtained by injecting a hyperpolarizing constant square-wave current pulse (100 ms duration) into the muscle fiber through the current electrode and by recording the resulting voltage deflection with a second microelectrode inserted at two distances from the current electrode. The current pulse generation, the acquisition of the voltage records and the calculation of the fiber constants were done in real time under computer control as described elsewhere.[30] The reciprocal of R_m from each fiber in normal physiological solution was the total membrane conductance (gm), and the same parameter measured in chloride free solution was the potassium conductance (gK). The mean chloride conductance (gCl) was estimated as the mean gm minus the mean gK. The compounds **1**, ***S*-2**, ***S*-4**, fenofibric acid, and clofibric acid, dissolved in dimethyl sulfoxide (DMSO), were applied in vitro on muscle bath, and gm and gK were measured before and 30 min after addition of increasing concentrations of each compound. The maximal concentration of DMSO used (0.5%) was without effect on the parameters studied.

Acknowledgment. This work was accomplished thanks to the financial support of the Ministero dell'Istruzione, dell'Università e della Ricerca (MIUR 2005033023) and Università degli Studi di Bari (Research Fund 2008).

Supporting Information Available: Spectroscopic data for intermediates and final compounds; statistics of crystallographic data and refinement; figures. This material is available free of charge via the Internet at http://pubs.acs.org.

References

(1) Elisaf, M. Effects of fibrates on serum metabolic parameters. *Curr. Med. Res. Opin.* **2002**, *18*, 269–276.
(2) Staels, B.; Dallongeville, J.; Auwerx, J.; Schoonjans, K.; Leitersdorf, E.; Fruchart, J.-C. Mechanism of action of fibrates on lipid and lipoprotein metabolism. *Circulation* **1998**, *98*, 2088–2093.
(3) Campbell, I. W. The Clinical Significance of PPAR Gamma Agonism. *Curr. Mol. Med.* **2005**, *5*, 349–363.
(4) Sprecher, D. L. Lipids, lipoproteins, and peroxisome proliferator activated receptor-delta. *Am. J. Cardiol.* **2007**, *100*, n20–n24.
(5) Sprecher, D. L.; Massien, C.; Pearce, G.; Billin, A. N.; Perlstein, I.; Willson, T. M.; Hassall, D. G.; Ancellin, N.; Patterson, S. D.; Lobe, D. C.; Johnson, T. G. Triglyceride: high-density lipoprotein cholesterol effects in healthy subjects administered a peroxisome proliferator activated receptor delta agonist. *Arterioscler. Thromb. Vasc. Biol.* **2007**, *27*, 359–365.
(6) Reilly, S. M.; Lee, C. H. PPAR delta as a therapeutic target in metabolic disease. *FEBS Lett.* **2008**, *582*, 26–31.
(7) Madrazo, J. A.; Kelly, D. P. The PPAR trio: regulators of myocardial energy metabolism in health and disease. *J. Mol. Cell. Cardiol.* **2008**, *44*, 968–975.
(8) Schmuth, M.; Jiang, Y. J.; Dubrac, S.; Elias, P. M.; Feingold, K. R. Thematic review series: skin lipids. Peroxisome proliferator-activated receptors and liver X receptors in epidermal biology. *J. Lipid Res.* **2008**, *49*, 499–509.
(9) Iwashita, A.; Muramatsu, Y.; Yamazaki, T.; Muramoto, M.; Kita, Y.; Yamazaki, S.; Mihara, K.; Moriguchi, A.; Matsuoka, N. Neuroprotective efficacy of the peroxisome proliferator-activated receptor delta-selective agonists in vitro and in vivo. *J. Pharmacol. Exp. Ther.* **2007**, *320*, 1087–1096.
(10) Peters, J. M.; Hollingshead, H. E.; Gonzalez, F. J. Role of peroxisome-proliferator-activated receptor beta/delta (PPARbeta/delta) in gastrointestinal tract function and disease. *Clin. Sci. (London)* **2008**, *115*, 107–127.
(11) Reifel Miller, A. Today's challenges and tomorrow's opportunities: ligands to Peroxisome Proliferator-Activated Receptors as Therapies for Type 2 Diabetes and Metabolic Syndrome. *Drug. Dev. Res.* **2006**, *67*, 574–578.
(12) Willson, T. M.; Brown, P. J.; Sternbach, D. D.; Henke, B. R. The PPARs: from orphan receptors to drug discovery. *J. Med. Chem.* **2000**, *43*, 527–550.
(13) Henke, B. R. Peroxisome proliferator-activated receptor alpha/gamma dual agonists for the treatment of type 2 diabetes. *J. Med. Chem.* **2004**, *47*, 4118–4127.
(14) Lehmann, J. M.; Moore, L. B.; Smith-Oliver, T. A.; Wilkison, W. O.; Willson, T. M.; Kliewer, S. A. An antidiabetic thiazolidinedione is a high affinity ligand for peroxisome proliferator-activated receptor gamma (PPAR gamma). *J. Biol. Chem.* **1995**, *270*, 12953–12956.
(15) Willson, T. M.; Cobb, J. E.; Cowan, D. J.; Wiethe, R. W.; Correa, I. D.; Prakash, S. R.; Beck, K. D.; Moore, L. B.; Kliewer, S. A.; Lehmann, J. M. The structure−activity relationship between peroxisome proliferator-activated receptor gamma agonism and the antihyperglycemic activity of thiazolidinediones. *J. Med. Chem.* **1996**, *39*, 665–668.
(16) Lohray, B. B.; Lohray, V. B.; Bajji, A. C.; Kalchar, S.; Poondra, R. R.; Padakanti, S.; Chakrabarti, R.; Vikramadithyan, R. K.; Misra, P.;

Juluri, S.; Mamidi, N. V.; Rajagopalan, R. (−)3-[4-[2-(Phenoxazin-10-yl)ethoxy]phenyl]-2-ethoxypropanoic acid [(−)DRF 2725]: a dual PPAR agonist with potent antihyperglycemic and lipid modulating activity. *J. Med. Chem.* **2001**, *44*, 2675–2678.
(17) Sauerberg, P.; Pettersson, I.; Jeppesen, L.; Bury, P. S.; Mogensen, J. P.; Wassermann, K.; Brand, C. L.; Sturis, J.; Woldike, H. F.; Fleckner, J.; Andersen, A. S.; Mortensen, S. B.; Svensson, L. A.; Rasmussen, H. B.; Lehmann, S. V.; Polivka, Z.; Sindelar, K.; Panajotova, V.; Ynddal, L.; Wulff, E. M. Novel tricyclic-alpha-alkyloxyphenylpropionic acids: dual PPARalpha/gamma agonists with hypolipidemic and antidiabetic activity. *J. Med. Chem.* **2002**, *45*, 789–804.
(18) Ebdrup, S.; Pettersson, I.; Rasmussen, H. B.; Deussen, H. J.; Frost Jensen, A.; Mortensen, S. B.; Fleckner, J.; Pridal, L.; Nygaard, L.; Sauerberg, P. Synthesis and biological and structural characterization of the dual-acting peroxisome proliferator-activated receptor alpha/gamma agonist ragaglitazar. *J. Med. Chem.* **2003**, *46*, 1306–1317.
(19) Devasthale, P. V.; Chen, S.; Jeon, Y.; Qu, F.; Shao, C.; Wang, W.; Zhang, H.; Cap, M.; Farrelly, D.; Golla, R.; Grover, G.; Harrity, T.; Ma, Z.; Moore, L.; Ren, J.; Seethala, R.; Cheng, L.; Sleph, P.; Sun, W.; Tieman, A.; Wetterau, J. R.; Doweyko, A.; Chandrasena, G.; Chang, S. Y.; Humphreys, W. G.; Sasseville, V. G.; Biller, S. A.; Ryono, D. E.; Selan, F.; Hariharan, N.; Cheng, P. T. Design and synthesis of *N*-[(4-methoxyphenoxy)carbonyl]-*N*-[[4-[2-(5-methyl-2-phenyl-4-oxazolyl)ethoxy]phenyl]methyl]glycine [Muraglitazar/BMS-298585], a novel peroxisome proliferator-activated receptor alpha/gamma dual agonist with efficacious glucose and lipid-lowering activities. *J. Med. Chem.* **2005**, *48*, 2248–2250.
(20) Koyama, H.; Miller, D. J.; Boueres, J. K.; Desai, R. C.; Jones, A. B.; Berger, J. P.; MacNaul, K. L.; Kelly, L. J.; Doebber, T. W.; Wu, M. S.; Zhou, G.; Wang, P. R.; Ippolito, M. C.; Chao, Y. S.; Agrawal, A. K.; Franklin, R.; Heck, J. V.; Wright, S. D.; Moller, D. E.; Sahoo, S. P. (2*R*)-2-ethylchromane-2-carboxylic acids: discovery of novel PPARalpha/gamma dual agonists as antihyperglycemic and hypolipidemic agents. *J. Med. Chem.* **2004**, *47*, 3255–3263.
(21) Shi, G. Q.; Dropinski, J. F.; McKeever, B. M.; Xu, S.; Becker, J. W.; Berger, J. P.; MacNaul, K. L.; Elbrecht, A.; Zhou, G.; Doebber, T. W.; Wang, P.; Chao, Y. S.; Forrest, M.; Heck, J. V.; Moller, D. E.; Jones, A. B. Design and synthesis of alpha-aryloxyphenylacetic acid derivatives: a novel class of PPARalpha/gamma dual agonists with potent antihyperglycemic and lipid modulating activity. *J. Med. Chem.* **2005**, *48*, 4457–4468.
(22) Ljung, B.; Bamberg, K.; Dahllof, B.; Kjellstedt, A.; Oakes, N. D.; Ostling, J.; Svensson, L.; Camejo, G. AZ 242, a novel PPARalpha/gamma agonist with beneficial effects on insulin resistance and carbohydrate and lipid metabolism in ob/ob mice and obese Zucker rats. *J. Lipid Res.* **2002**, *43*, 1855–1863.
(23) Grey, A. Skeletal consequences of thiazolidinedione therapy. *Osteoporosis Int.* **2008**, *19*, 129–137.
(24) Rubenstrunk, A.; Hanf, R.; Hum, D. W.; Fruchart, J.-C.; Staels, B. Safety issues and prospects for future generations of PPAR modulators. *Biochim. Biophys. Acta* **2007**, *1771*, 1065–1081.
(25) Shearer, B. G.; Billin, A. N. The next generation of PPAR drugs: do we have the tools to find them? *Biochim. Biophys. Acta* **2007**, *1771*, 1082–1093.
(26) Montanari, R.; Saccoccia, F.; Scotti, E.; Crestani, M.; Godio, C.; Gilardi, F.; Loiodice, F.; Fracchiolla, G.; Laghezza, A.; Tortorella, P.; Lavecchia, A.; Novellino, E.; Mazza, F.; Aschi, M.; Pochetti, G. Crystal structure of the peroxisome proliferator-activated receptor gamma (PPARgamma) ligand binding domain complexed with a novel partial agonist: a new region of the hydrophobic pocket could be exploited for drug design. *J. Med. Chem.* **2008**, *51*, 7768–7776.
(27) Feller, D. R.; Kamanna, V. S.; Newman, H. A.; Romstedt, K. J.; Witiak, D. T.; Bettoni, G.; Bryant, S. H.; Conte-Camerino, D.; Loiodice, F.; Tortorella, V. Dissociation of hypolipidemic and antiplatelet actions from adverse myotonic effects of clofibric acid related enantiomers. *J. Med. Chem.* **1987**, *30*, 1265–1267.
(28) Bettoni, G.; Loiodice, F.; Tortorella, V.; Conte-Camerino, D.; Mambrini, M.; Ferrannini, E.; Bryant, S. H. Stereospecificity of the chloride ion channel: the action of chiral clofibric acid analogues. *J. Med. Chem.* **1987**, *30*, 1267–1270.
(29) Hodel, C. Myopathy and rhabdomyolysis with lipid-lowering drugs. *Toxicol. Lett.* **2002**, *128*, 159–168.
(30) Pierno, S.; Didonna, M. P.; Cippone, V.; De Luca, A.; Pisoni, M.; Frigeri, A.; Nicchia, G. P.; Svelto, M.; Chiesa, G.; Sirtori, C.; Scanziani, E.; Rizzo, C.; De Vito, D.; Conte Camerino, D. Effects of chronic treatment with statins and fenofibrate on rat skeletal muscle: a biochemical, histological and electrophysiological study. *Br. J. Pharmacol.* **2006**, *149*, 909–919.
(31) Liang, Y.; Xie, Y. X.; Li, J. H. Modified palladium-catalyzed Sonogashira cross-coupling reactions under copper-, amine-, and solvent-free conditions. *J. Org. Chem.* **2006**, *71*, 379–381.
(32) Bhanushali, M. J.; Nandurkar, N. S.; Bhor, M. D.; Bhanage, B. M. Direct reductive amination of carbonyl compounds using bis(triphenylphosphine)copper(I) tetrahydroborate. *Tetrahedron Lett.* **2007**, *48*, 1273–1276.
(33) Tarzia, G.; Duranti, A.; Tontini, A.; Piersanti, G.; Mor, M.; Rivara, S.; Plazzi, P. V.; Park, C.; Kathuria, S.; Piomelli, D. Design, synthesis, and structure−activity relationships of alkylcarbamic acid aryl esters, a new class of fatty acid amide hydrolase inhibitors. *J. Med. Chem.* **2003**, *46*, 2352–2360.
(34) Pinelli, A.; Godio, C.; Laghezza, A.; Mitro, N.; Fracchiolla, G.; Tortorella, V.; Lavecchia, A.; Novellino, E.; Fruchart, J. C.; Staels, B.; Crestani, M.; Loiodice, F. Synthesis, biological evaluation, and molecular modeling investigation of new chiral fibrates with PPARalpha and PPARgamma agonist activity. *J. Med. Chem.* **2005**, *48*, 5509–5519.
(35) Kleywegt, G. J.; Zou, J. Y.; Kjeldgaard, M.; Jones, T. A. Around O. In *International Tables for Crystallography, Vol. F. Crystallography of Biological Macromolecules*; Rossmann, M. G., Arnold, E., Eds.; Kluwer Academic Publishers: Dordrecht, The Netherlands, 2001, pp 353−356, 366−367.
(36) Meyer, E. A.; Castellano, R. K.; Diederich, F. Interactions with aromatic rings in chemical and biological recognition. *Angew. Chem., Int. Ed.* **2003**, *42*, 1210–1250.
(37) Kawatkar, S. P.; Kuntz, D. A.; Woods, R. J.; Rose, D. R.; Boons, G. J. Structural basis of the inhibition of Golgi alpha-mannosidase II by mannostatin A and the role of the thiomethyl moiety in ligand−protein interactions. *J. Am. Chem. Soc.* **2006**, *128*, 8310–8319.
(38) Wang, W.; Devasthale, P.; Farrelly, D.; Gu, L.; Harrity, T.; Cap, M.; Chu, C.; Kunselman, L.; Morgan, N.; Ponticiello, R.; Zebo, R.; Zhang, L.; Locke, K.; Lippy, J.; O'Malley, K.; Hosagrahara, V.; Kadiyala, P.; Chang, C.; Muckelbauer, J.; Doweyko, A. M.; Zahler, R.; Ryono, D.; Hariharan, N.; Cheng, P. T. Discovery of azetidinone acids as conformationally-constrained dual PPARalpha/gamma agonists. *Bioorg. Med. Chem. Lett.* **2008**, *18*, 1939–1944.
(39) *GOLD, version 4.0*; CCDC Software Limited: Cambridge, U.K., 2008.
(40) Jones, G.; Willett, P.; Glen, R. C.; Leach, A. R.; Taylor, R. Development and validation of a genetic algorithm for flexible docking. *J. Mol. Biol.* **1997**, *267*, 727–748.
(41) Schulz-Gasch, T.; Stahl, M. Binding site characteristics in structure-based virtual screening: evaluation of current docking tools. *J. Mol. Model.* **2003**, *9*, 47–57.
(42) Wang, R.; Lu, Y.; Wang, S. Comparative evaluation of 11 scoring functions for molecular docking. *J. Med. Chem.* **2003**, *46*, 2287–2303.
(43) Kellenberger, E.; Rodrigo, J.; Muller, P.; Rognan, D. Comparative evaluation of eight docking tools for docking and virtual screening accuracy. *Proteins* **2004**, *57*, 225–242.
(44) Warren, G. L.; Andrews, C. W.; Capelli, A. M.; Clarke, B.; LaLonde, J.; Lambert, M. H.; Lindvall, M.; Nevins, N.; Semus, S. F.; Senger, S.; Tedesco, G.; Wall, I. D.; Woolven, J. M.; Peishoff, C. E.; Head, M. S. A critical assessment of docking programs and scoring functions. *J. Med. Chem.* **2006**, *49*, 5912–5931.
(45) Verdonk, M. L.; Cole, J. C.; Hartshorn, M. J.; Murray, C. W.; Taylor, R. D. Improved protein−ligand docking using GOLD. *Proteins* **2003**, *52*, 609–623.
(46) Eldridge, M. D.; Murray, C. W.; Auton, T. R.; Paolini, G. V.; Mee, R. P. Empirical scoring functions: I. The development of a fast empirical scoring function to estimate the binding affinity of ligands in receptor complexes. *J. Comput.-Aided Mol. Des.* **1997**, *11*, 425–445.
(47) Rimon, D.; Ludatscher, R.; Cohen, L. Clofibrate-induced muscular syndrome. Case report with ultrastructural findings and review of the literature. *Isr. J. Med. Sci.* **1984**, *20*, 1082–1086.
(48) Pierce, L. R.; Wysowski, D. K.; Gross, T. P. Myopathy and rhabdomyolysis associated with lovastatin−gemfibrozil combination therapy. *JAMA, J. Am. Med. Assoc.* **1990**, *264*, 71–75.
(49) Langer, T.; Levy, R. I. Acute muscular syndrome associated with administration of clofibrate. *N. Engl. J. Med.* **1968**, *279*, 856–858.
(50) Reaven, P.; Witztum, J. L. Lovastatin, nicotinic acid, and rhabdomyolysis. *Ann. Intern. Med.* **1988**, *109*, 597–598.
(51) Hodel, C. M.; Kruslin, E. Risk profile of lipid-lowering drugs. *Arh. Hig. Rada Toksikol.* **1997**, *48*, 67–86.
(52) Kruslin, E.; Hodel, C. M. Myotoxicity in lipid-lowering therapy. *Arh. Hig. Rada Toksikol.* **1997**, *48*, 7–26.
(53) Chauvin, M.; Zupan, M.; Brechenmacher, C. Sindrome musculaire atypique avec myolyse au cours d'un traitement chronique par fibrates (Atypical muscle syndrome characterized by myolysis

during a chronic treatment with fibrates). *Arch. Mal. Coeur. Vaiss.* **1988**, *81*, 921–923.
(54) Bermingham, R. P.; Whitsitt, T. B.; Smart, M. L.; Nowak, D. P.; Scalley, R. D. Rhabdomyolysis in a patient receiving the combination of cerivastatin and gemfibrozil. *Am. J. Health Syst. Pharm.* **2000**, *57*, 461–464.
(55) Pierno, S.; Camerino, G. M.; Cippone, V.; Rolland, J. F.; Desaphy, J. F.; De Luca, A.; Liantonio, A.; Bianco, G.; Kunic, J. D.; George, A. L., Jr.; Conte Camerino, D. Statins and fenofibrate affect skeletal muscle chloride conductance in rats by differently impairing ClC-1 channel regulation and expression. *Br. J. Pharmacol.* **2009**, *156*, 1206–1215.
(56) Pochetti, G.; Godio, C.; Mitro, N.; Caruso, D.; Galmozzi, A.; Scurati, S.; Loiodice, F.; Fracchiolla, G.; Tortorella, P.; Laghezza, A.; Lavecchia, A.; Novellino, E.; Mazza, F.; Crestani, M. Insights into the mechanism of partial agonism: crystal structures of the peroxisome proliferator-activated receptor gamma ligand-binding domain in the complex with two enantiomeric ligands. *J. Biol. Chem.* **2007**, *282*, 17314–17324.
(57) Leslie, A. G. W. *Jt. CCP4 ESF-EACMB Newlett. Protein Crystallogr.* **1992**, 26.
(58) Brunger, A. T.; Adams, P. D.; Clore, G. M.; DeLano, W. L.; Gros, P.; Grosse-Kunstleve, R. W.; Jiang, J. S.; Kuszewski, J.; Nilges, M.; Pannu, N. S.; Read, R. J.; Rice, L. M.; Simonson, T.; Warren, G. L. Crystallography NMR system: a new software suite for macromolecular structure determination. *Acta Crystallogr., Sect. D: Biol. Crystallogr.* **1998**, *54* (Part 5), 905–921.
(59) *Molecular Operating Environment* (*MOE*), *version 2005.06*; Chemical Computing Group, Inc.: Montreal, Canada, 2005.
(60) Huang, C. C.; Couch, G. S.; Pettersen, E. F.; Ferrin, T. E. Chimera: an extensible molecular modeling application constructed using standard components. *Pac. Symp. Biocomput.* **1996**, *1*, 724, http://www.cgl.ucsf.edu/chimera
(61) Case, D. A.; Darden, T. A.; Cheatham, T. E., III; Simmerling, C. L.; Wang, J.; Duke, R. E.; Luo, R.; Merz, K. M.; Pearlman, D. A.; Crowley, M.; Walker, R. C.; Zhang, W.; Wang, B.; Hayik, S.; Roitberg, A.; Seabra, G.; Wong, K. F.; Paesani, F.; Wu, X.; Brozell, S.; Tsui, V.; Gohlke, H.; Yang, L.; Tan, C.; Mongan, J.; Hornak, V.; Cui, G.; Beroza, P.; Mathews, D. H.; Schafmeister, C.; Ross, W. S.; Kollman, P. A. *AMBER 9*; University of California, San Francisco, 2006.
(62) Cornell, W. D.; Cieplak, P.; Bayly, C. I.; Gould, I. R.; Merz, K. M.; Ferguson, D. M.; Spellmeyer, D. C.; Fox, T.; Caldwell, J. W.; Kollman, P. A. A second generation force field for the simulation of proteins, nucleic acids, and organic molecules. *J. Am. Chem. Soc.* **1995**, *117*, 5179–5197.
(63) Bernstein, F. C.; Koetzle, T. F.; Williams, G. J.; Meyer, E. F., Jr.; Brice, M. D.; Rodgers, J. R.; Kennard, O.; Shimanouchi, T.; Tasumi, M. The Protein Data Bank: a computer-based archival file for macromolecular structures. *J. Mol. Biol.* **1977**, *112*, 535–542.
(64) Raspe, E.; Madsen, L.; Lefebvre, A. M.; Leitersdorf, I.; Gelman, L.; Peinado-Onsurbe, J.; Dallongeville, J.; Fruchart, J. C.; Berge, R.; Staels, B. Modulation of rat liver apolipoprotein gene expression and serum lipid levels by tetradecylthioacetic acid (TTA) via PPARalpha activation. *J. Lipid Res.* **1999**, *40*, 2099–2110.
(65) Hollon, T.; Yoshimura, F. K. Variation in enzymatic transient gene expression assays. *Anal. Biochem.* **1989**, *182*, 411–418.